

# Evaluating Activator-Inhibitor Mechanisms for Sensors Coordination

Giovanni Neglia  
INRIA, Sophia Antipolis, France  
Università degli Studi di Palermo, Italia  
giovanni.neglia@ieee.org

Giuseppe Reina  
Università degli Studi di Catania, Italia  
g.reina@gmail.com

## ABSTRACT

The possibility to employ reaction-diffusion models to build spatial patterns in sensor networks has been advocated in other works. Nevertheless it has not been investigated how the biologically-inspired solutions perform in comparison to more traditional ones taking into account specificities of sensor networks like severe energy constraints. In this paper we present some preliminary results on the comparison between a biologically inspired coordination mechanism based on activator-inhibitor interaction and a simple mechanism, where nodes do not communicate but activate their sensing circuitry according to some probability.

## Keywords

Sensor networks, sensor coordination, bio-inspired mechanisms, reaction-diffusion models, activator-inhibitor models.

## 1. INTRODUCTION

One of the challenges of sensor networks is the development of long-lived sensor networks in spite of energy constraints of individual nodes. Depending on the specific application (type and frequency of the events to capture, size of the network) the main energy consuming activity can either be sensing or communication. In order to spare energy, nodes can periodically turn off their sensing circuitry or their radio. In both cases coordination among nodes is needed. In fact nodes can stop sensing only if other nodes in the neighborhood guarantee an adequate coverage of the area to sense<sup>1</sup>. At the same time sensor networks usually rely on multi-hop communications where sensors relay data produced by other sensors to one or more data sinks. So powering down radios on sensor nodes makes such nodes unavailable for multi-hop communication. Again coordination

<sup>1</sup>Usually the number of nodes deployed is significantly higher than the minimum needed, in order to make up for random deployment and failures.

Permission to make digital or hard copies of all or part of this work for personal or classroom use is granted without fee provided that copies are not made or distributed for profit or commercial advantage and that copies bear this notice and the full citation on the first page. To copy otherwise, to republish, to post on servers or to redistribute to lists, requires prior specific permission and/or a fee.

*Bionetics* '07, December 10-13, 2007, Budapest, Hungary  
Copyright 2007 ICST 978-963-9799-11-0.

among nodes is needed in order to maintain communication backbones in the sensor network.

This coordination could theoretically be managed by a central authority which sends specific commands to each single node, but in most cases this approach is unfeasible for large sensor networks. In fact sensors are often randomly deployed, are exposed to hostile environments, can exhaust their batteries, moreover communication is subject to the vagaries of the wireless channel. All these issues lead to dynamics much faster than those of wired networks, hard to manage in a centralized way. Besides central management could impose on the network a high cost in terms of bandwidth and energy for communication. So the network should be self-organizing, i.e. nodes should autonomously carry out measurement and adaptive configuration.

Many protocols addressing the issue of node coordination have been proposed (see [5] and references there). In this paper we propose a new coordination mechanism for sensing activity based on activator-inhibitor interaction, a model used to explain pattern formation in biological system, e.g. how identical totipotent cells can differentiate in the different parts of an organism [8].

The idea to use pattern formation models in sensor networks is not completely new. For example in [6], and some subsequent papers of Thomas Henderson, reaction-diffusion models are proposed to build a spatial pattern that could help robot operation in a given area. Research in amorphous computing [1] has been recently looking at sensor networks as a instantiation of an amorphous computer [3]. The focus of such research is mainly on developing robust primitives, appropriate methods for analysis, and designing new high-level programming languages.

Despite this research activity, to the best of our knowledge, it has not been investigated how new biologically-inspired solutions for sensor networks perform in comparison to more traditional ones. In this paper we present some preliminary results on the comparison between a coordination mechanism based on activator-inhibitor interaction and a simpler one, where nodes do not communicate but activate their sensing circuitry according to some probability.

Our preliminary results suggest that the biologically inspired mechanism is able to significantly reduce energy consumption for sensing purpose, but more investigation is needed to take into account increased communication costs.

The paper is organized as follows. In Sec. 2 we illustrate the specific coordination problem we want to address. In Sec. 3 and in Sec. 4 we respectively present the new biologically inspired coordination mechanism and the probabilistic

one. In Sec. 5 the performances of the two mechanisms are compared. Conclusions and future research activity are in Sec. 6.

## 2. NETWORK SCENARIO

We consider  $N$  wireless sensors deployed uniformly at random in an area  $A$ . The communication model is simple: two sensors can communicate if their distance is smaller than  $r$ , the radio transmission range of each sensor. The network is quite dense, i.e. each sensor has many other sensors in its transmission range.

We assume that the most energy-consuming activity is sensing, because of power requirement of sensing circuitry or computation required to process data<sup>2</sup>. For this reason, we would like some nodes to turn off their sensing circuitry in order to spare battery and increase sensor network lifetime. We assume that each node can sense up to a distance  $d$ , where  $d \gg r$ . As we are going to discuss in the following section, for  $d < r$  an activator-inhibitor scheme would require nodes to be able to estimate distances from other nodes. Sensing coverage ( $\alpha$ ) is evaluated as the fraction of the area  $A$  where events are sensed by at least one sensor.

## 3. THE ACTIVATOR-INHIBITOR MECHANISM

Activator-inhibitor models have been able to explain spatial concentration patterns with characteristic features known from biological systems: in this case a strong short range positive feedback -usually referred to as autocatalysis- is coupled with a long range negative feedback -usually referred to as lateral inhibition. Their interaction can produce polar and periodic patterns as well as net-like structures, able to adapt to disturbances while preserving some specific distances between activity centers. Both differential equation and cellular automata modeling approaches have been successfully applied to these systems (e.g. [8] and [4]).

Our starting point is the differential equation model in [8]. Let say  $a(x, y, t)$  and  $h(x, y, t)$  respectively activator and inhibitor densities in the area  $A$ . The following set of equations with zero flux boundary conditions can produce periodical patterns for specific values of the parameters:

$$\begin{cases} \frac{\partial a}{\partial t} = \frac{ca^2}{h} - \mu a + \rho_0 + D_a \nabla^2 a, \\ \frac{\partial h}{\partial t} = ca^2 - \nu h + \rho_1 + D_h \nabla^2 h, \\ \mathbf{n} \cdot \nabla a = 0 \text{ on } \partial A, \\ \mathbf{n} \cdot \nabla h = 0 \text{ on } \partial A, \end{cases} \quad (1)$$

where  $\nabla f$  and  $\nabla^2 f$  respectively denote the gradient and the laplacian of function  $f$ , and  $\partial A$  the boundary of the area  $A$ . A possible stationary solution (i.e. which does not depend on time  $t$ ) of equation system (1) on a unitary area is shown in Figure 1. Both inhibitor and activator densities (respectively represented by the meshed and the not-meshed surface) exhibit a periodic pattern. The inhibitor density varies over a narrower range than the activator density. This happens because the inhibitor diffuses faster than the activator ( $D_h > D_a$ ). This condition is necessary to

<sup>2</sup>Some illustrative costs from [7]: a photocell can absorb about 1 mW, transmission can require 1  $\mu$ J per bit and execution of an instruction 0.01  $\mu$ J.

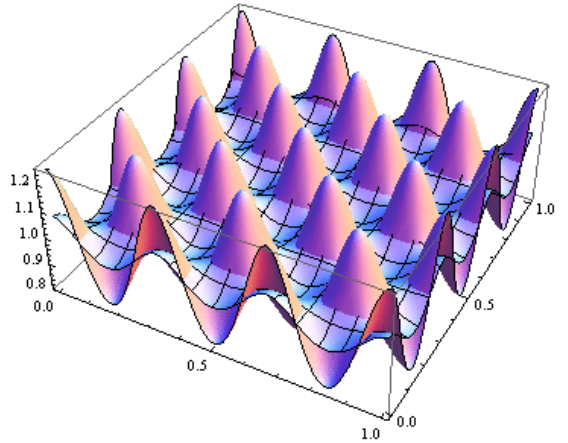


**Figure 1: An example of a stationary solution of equation system (1): the meshed surface represents the inhibitor, the other surface the activator.**

have non-homogeneous patterns and corresponds to the long range versus short range characteristics of the two different feedbacks.

In biological systems high levels of activator concentration can activate other processes in cells. Hence this mechanism can explain how differentiation can arise in a group of originally identical cells. We would like to use the same mechanism to differentiate sensor status. In order to achieve this purpose we will let the sensor field operate as a discrete approximation, in space and in time, of equation system (1). In our algorithm, each sensor, say  $i$ , stores its own activator and inhibitor values (respectively  $a_i$  and  $h_i$ ) and it broadcasts them every  $\tau$  seconds. With the same periodicity sensor  $i$  updates its own concentration values on the basis of the information collected from its neighbours (let  $N_i$  denote this set) according to the following equations, which can be derived from a discretization of equation system (1):

$$\begin{cases} a_i(t_{k+1}) = a_i(t_k) + \tau \left( \frac{ca_i^2}{h} - \mu a_i + \rho_0 + \frac{9D_a}{4r^2} \sum_{j \in N_i} (a_{j,i}(t_{k+1}) - a_i(t_k)) \right), \\ h_i(t_{k+1}) = h_i(t_k) + \tau \left( ca_i^2 - \nu h_i + \rho_1 + \frac{9D_h}{4r^2} \sum_{j \in N_i} (h_{j,i}(t_{k+1}) - h_i(t_k)) \right), \end{cases} \quad (2)$$

where  $t_{k+1} = t_k + \tau$  and  $a_{j,i}(t)$  and  $h_{j,i}(t)$  denote the concentration values of sensor  $j$  known from sensor  $i$  at time  $t$ . Sensors, whose activator concentration is above a given threshold ( $a_{th}$ ) and is the highest value among the neighbours, become active turning on their sensing circuitry.

**Remarks.** Note that the zero flux boundary conditions are intrinsically satisfied because the algorithm simply redistribute activator and inhibitor among sensors in the network. We observe also that this mechanism can work only for  $d \gg r$ . In fact for  $d < r$  we should have many active

sensors in the neighborhood of a node in order to guarantee adequate coverage. This would require activator and inhibitor concentrations to vary significantly in this area, but this is not possible as long as each sensor simply average its neighbours concentration values as in Eq. (2).

### Activator-Inhibitor Mechanism Configuration.

In this section we address the configuration of the proposed mechanism, i.e. how to choose parameters in Eq. (2) in order to create the desired pattern with active sensors equidistant from each other and able to guarantee an adequate coverage of the area.

Our starting point is the continuous model in equation system (1). In [9] conditions are provided to guarantee the emergence of patterns for a generic reaction-diffusion system, imposing the stability of homogenous solutions and the existence of unstable not-homogeneous solutions. To use the notation in [9], equation system (1) can be rewritten as:

$$\begin{aligned}\frac{\partial a}{\partial t} &= f(a, h) + D_a \nabla^2 a, \\ \frac{\partial h}{\partial t} &= g(a, h) + D_h \nabla^2 h.\end{aligned}$$

where  $f(a, h) = ca^2/h - \mu a + \rho_0$  and  $g(a, h) = ca^2 - \nu a + \rho_1$ . We carry the stability analysis at a homogeneous steady state solution,  $(a(x, y, t), h(x, y, t)) = (a_0, h_0)$ , which is a positive solution of:

$$\begin{aligned}f(a_0, h_0) &= \frac{ca_0^2}{h_0} - \mu a_0 + \rho_0 = c - \mu + \rho_0 = 0 \\ g(a_0, h_0) &= ca_0^2 - \nu h_0 + \rho_1 = c - \nu + \rho_1 = 0\end{aligned}$$

Being that we are designing the mechanism, we can choose  $(a_0, h_0) = (1, 1)$ . Let  $f_a$  be the partial derivative of  $f$  with respect to  $a$  evaluated at  $(a_0, h_0)$ .

Linearizing around the steady state  $(a_0, h_0)$  we obtain that the general solution for  $\mathbf{w}(x, y, t) = (a(x, y, t) - a_0, h(x, y, t) - h_0)$  is [9]:

$$\mathbf{w}(x, y, t) = \sum_k \left( c_{k,1} e^{\lambda_{k,1} t} + c_{k,2} e^{\lambda_{k,2} t} \right) \mathbf{W}_k(x, y)$$

where  $\mathbf{W}_k(x, y)$  is an eigenfunction corresponding to the eigenvalue  $k^2$  of the following problem:

$$\begin{cases} \nabla^2 \mathbf{W}_k(x, y) = -k^2 \mathbf{W}_k(x, y), \\ (n \cdot \nabla) \mathbf{W}_k(x, y) = 0, \end{cases}$$

and  $\lambda_{k,1}, \lambda_{k,2}$  are the roots of the following equation:

$$\lambda^2 + \lambda[k^2(D_a + D_h) - (f_a + g_h)] + h(k^2) = 0, \quad (3)$$

where  $h(k^2) = k^4 D_a D_h - k^2(D_a g_h + D_h f_a) + (f_a g_h - g_a f_h)$ .

The steady state  $(a_0, h_0)$  is linearly stable if both solutions of Eq. (3) have  $\text{Re}(\lambda_k) < 0$  for  $k^2 = 0$ . For the steady state to be unstable to spatial disturbances we require  $\text{Re}(\lambda_k) > 0$  for some  $k \neq 0$ . The values of  $k^2$  corresponding to unstable modes are those eigenvalues for which  $h(k^2) < 0$ . The following inequalities can be derived [9]:

$$\begin{cases} f_a + g_h < 0, \\ f_a g_h - f_h g_a > 0, \\ D_h f_a + D_a g_h > 0, \\ (D_h f_a + D_a g_h)^2 - 4D_a D_h (f_a g_h - f_h g_a) > 0. \end{cases} \quad (4)$$

The first two inequalities guarantee linear stability of the steady state, the other two the existence of non-homogeneous unstable modes. For equation system (1), conditions (4) are:

$$\begin{cases} 2c - \mu - \nu < 0, \\ 2c^2 - (2c - \mu)\nu > 0, \\ D_h(2c - \mu) - D_a \nu > 0, \\ \nu^2 D_a^2 - 2(4c^2 - 2c\nu + \mu\nu)D_a D_h + (-2c + \mu)^2 D_h^2 \end{cases} \quad (5)$$

and  $h(k^2)$  has the following expression  $h(k^2) = D_a D_h k^4 - (D_h(2c - \mu) - D_a \nu)k^2 + 2c^2 - (2c - \mu)\nu$ .

Conditions (4) do not determine the distance between activator maxima. In order to control this distance we would like to add more conditions to have a single spatially-periodic unstable mode that should guarantee a fixed distance among activator maxima and hence (hopefully) among active sensors. Considering a rectangular domain, with  $0 \leq x \leq L_x$  and  $0 \leq y \leq L_y$ , the following expressions hold for eigenvalues and eigenvectors:

$$\begin{aligned}k_{n,m}^2 &= \frac{n^2 \pi^2}{L_x^2} + \frac{m^2 \pi^2}{L_y^2} \\ \mathbf{W}_{\mathbf{k}_{n,m}}(x, y) &\propto \cos\left(\frac{n\pi x}{L_x}\right) \cos\left(\frac{m\pi y}{L_y}\right) \quad (6)\end{aligned}$$

where  $n$  and  $m$  are integers. Given  $n$  and  $m$  the distance between adjacent maxima is fixed and the number of maxima can be  $\lfloor (n+1)(m+1)/2 \rfloor$  or  $\lceil (n+1)(m+1)/2 \rceil$ . In our study we consider for simplicity a squared area. Moreover we want the same spatial period in both the dimension  $x$  and  $y$ , so we want  $n = m = n_0$ , selecting the eigenvalue  $k_c^2$ :

$$k_c^2 = k_{n_0, n_0}^2 = 2 \frac{n_0^2 \pi^2}{L^2}$$

In order to let only the corresponding mode be unstable, we can impose the following two conditions:

$$\begin{cases} \frac{D_h f_a + D_a g_h}{2D_a D_h} = k_c^2 \\ \sqrt{\frac{(D_h f_a + D_a g_h)^2 - 4D_a D_h (f_a g_h - f_h g_a)}{2D_a D_h}} < \frac{\pi^2}{L^2} \end{cases} \quad (7)$$

The first one imposes that  $k_c^2$  is the value for which  $h(k^2)$  is minimum (the vertex abscissa of the parabola individuated by  $h(k^2)$ ). The second one strongly limits the possibility for other modes to be excited imposing that the eigenvalue  $k_{n_0, n_0-1}^2$  corresponds to a stable mode, i.e.  $h(k_{n_0, n_0-1}^2) > 0$ . Note that this condition does not definitely exclude the existence of other unstable modes. For instance if  $n_0 = 5$  then  $k_c^2 = k_{5,5}^2 = 50\pi^2/L^2$ , but being that  $k_{7,1}^2 = k_{1,7}^2 = k_{5,5}^2$ , there can be also other unstable modes.

In our simulation we always observed the formation of non homogenous patterns with local maxima of activator density when conditions (5) are satisfied. On the other hand the number of local maxima is in general lower than the number determined by the eigenvalue  $k_c^2$  we select through conditions (7).

## 4. THE PROBABILISTIC MECHANISM

In the probabilistic coordination mechanism each node independently activates its sensing circuitry with probability

**Table 1: Network and mechanisms parameters**

network			
$A$	1x1	$N$	6125
$r$	0.0228	$d$	0.22
activator-inhibitor mechanism			
$\mu$	0.75	$\nu$	0.8
$D_a$	0.000222273	$D_h$	0.00580619
$\rho_0$	0.25	$\rho_1$	0.3
$c$	0.5	$\tau$	0.003
$a_{th}$	1.8		
probabilistic mechanism			
$p$	$p_1 = 0.416\%$ , $p_2 = 0.509\%$		

$p$ . This mechanism does not require any form of communication among nodes, but we can expect that more active sensor will be required in comparison to the activator-inhibitor mechanism in order to guarantee the same sensing coverage.

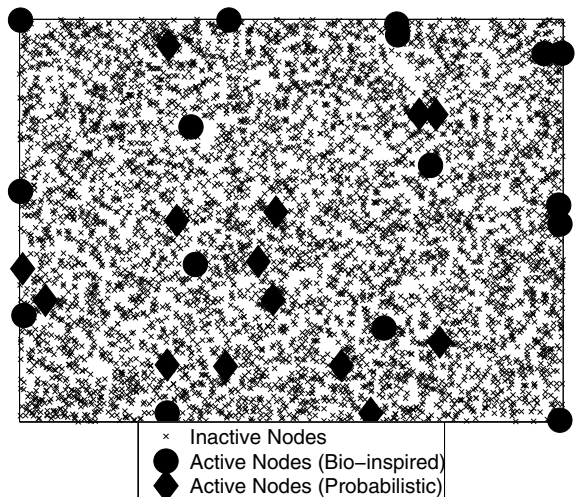
### Probabilistic Mechanism Configuration.

In order to determine the activation probability  $p$  for the probabilistic mechanism, we can use the following formula valid for the average coverage of an infinite Poisson field:  $\alpha = 1 - e^{-p\lambda\pi d^2}$  [10], where  $\lambda$  is node density ( $= N/L^2$  in our case). For a finite area this formula provides an upper bound for the coverage, because it also takes into account the contribution of eventual nodes outside the area. Hence it can be used to derive a lower bound for the actual probability  $p$  needed to guarantee the desired average coverage  $\alpha$ . The smaller  $d/L$ , the tighter the bound.

## 5. PERFORMANCE EVALUATION

We want to study which active sensor patterns arise with the two mechanisms and how efficient they are in terms of sensing coverage of the field and power consumption. In this section we present some preliminary results obtained through a Java simulator we developed starting from the Amorphous Gray-Scott simulator [2].

For the activator-inhibitor mechanism we chose  $n_0 = 6$ . All the parameters of the algorithm deriving from equation system (1) (i.e.  $D_a$ ,  $D_h$ ,  $\mu$ ,  $\nu$ ,  $\rho_0$ ,  $\rho_1$ ,  $c$ ) have been selected such that conditions (5) and the first of conditions (7) are satisfied and there is single unstable mode corresponding to  $k_c^2 = k_{n_0, n_0}^2$ . Concentrations at each node are initially set equiprobably to a high (1.8) or a low (0.2) concentration value. The activator threshold value  $a_{th}$  is set equal to 1.8. The area has been (without loss of generality) considered unitary, while the number of nodes  $N$  and the transmission range  $r$  have been selected imposing an average number of neighbours higher than 10 and a number of disjoint neighborhood (i.e. non overlapping circles of radius  $r$ ) in the area  $A$  higher than 121. These two conditions should let the sensor field well approximate the continuous model described by equation system (1). The first condition guarantees that the network is well connected and in particular that the probability of a sensor having no neighbours is very small, the second one guarantees that the desired distance between local maxima is larger than the transmission range, otherwise the concentration averaging operation at each node would not let emerge a periodic pattern. The time step  $\tau$  has been selected by trial and error has a large value still assuring


**Figure 2: Sensor activated by the two mechanisms.**

the emergence of the periodic pattern. Finally we have chosen the sensing range  $d$  in order to have a sensing coverage near to 95%. For the probabilistic mechanism two different values of the activation probability have been considered:  $p_1 = 0.416\%$  and  $p_2 = 0.509\%$ . They have been selected in order to achieve approximately the same performance of the activator-inhibitor mechanism, respectively in terms of average coverage probability ( $\alpha$ ) and minimum coverage guarantee in 90% of the cases ( $\alpha_{90\%}$ ). Table 1 shows the values of all the parameters.

We have generated 40 different sensor placements. For each of them we have simulated the activator-inhibitor mechanism and the probabilistic one, logging the final number of active nodes and their positions. For the activator-inhibitor mechanism, we have also logged the number of messages ( $M$ ) exchanged until the whole concentration varies less than  $0.008\tau$  between two consecutive global updates. Figure 2 shows exemplificative patterns of active sensors obtained with the two mechanisms.

Energy consumption for sensing purpose is clearly related to the number of active nodes. In particular we can evaluate it in two different ways. In the first case we just consider sensing cost to be proportional to the number of active sensors ( $S$  in Table 2). This corresponds to the case where the sensing field really coincides with the 1x1 area with  $N$  nodes we are simulating. In the second case we consider sensing cost to be proportional to an equivalent number of sensors (say it  $S_{eq}$ ) where each active node is weighted considering which fraction of its sensing area (a circle with radius  $d$  centered in the sensor) is inside the unitary area. This corresponds to consider an infinite sensing field with  $N$  sensors per area unit<sup>3</sup>. The difference among the two is significant due to border effects (see remarks below).

Table 2 shows average performance of the two mechanisms. The results show how sensing cost is much higher for the probabilistic algorithm. When our target is the average coverage (then we consider  $p_1$ ), the number of sensors activated is 100% higher in comparison to the activator-inhibitor

<sup>3</sup>Note that sensing coverage should be evaluated differently for the infinite field scenario taking into account that also nodes out of the unitary area contribute to its coverage.

**Table 2: Results (95% confidence intervals)**

	activator-inhibitor	probabilistic	
		$p_1$	$p_2$
$S$	[14.91,16.59]	[24.65,27.30]	[30.42,33.00]
$S_{eq}$	[9.87,11.18]	[20.04,22.06]	[25.04,27.10]
$\alpha$	[0.93,0.95]	[0.93,0.96]	[0.95,0.97]
$\alpha_{90\%}$	0.92	0.88	0.92
$M$	[90038,111880]	-	-

mechanism for the infinite field. The reaction-diffusion process proves to be able to space away the concentration maxima. The performance gap is smaller on the unitary field (only 60%). In fact, as we can note from Figure 2 and as it is predicted by the continuous model (Figure 1 and Eq. (6)) in reaction-diffusion systems many concentration maxima are on the boundaries of the area. These maxima correspond to active sensors which only partially contribute to the coverage of the unitary area (but they would contribute to the coverage of adjacent areas). This effect is particularly significant in cases where the number of sensors to be activated in the reference area is quite small (i.e. “large”  $d$  values). Finally when we consider minimum coverage guarantees, the activator-inhibitor algorithm offers even better performance. Probabilistic forwarding exhibits a much higher variability in placement of active nodes, so that the average number of active sensors with the probabilistic mechanism has to be from 100% up to 160% higher under the two scenarios in order to guarantee the same minimum coverage level.

## 6. CONCLUSIONS AND FUTURE RESEARCH

From the previous results it appears that the activator-inhibitor mechanism is able to spare energy for sensing purpose, activating a smaller number of sensors. At the same time Table 2 shows also that a high number of message is needed in order to establish the pattern starting from a clean slate status. Message exchange is needed until an almost stable configuration is reached and active nodes are individuated. Should nothing change, the initial communication cost would become negligible after a long enough network operation time. In reality active nodes can go out of battery or can undergo temporary failures. For this reason the algorithm should run continuously in order to keep track of the changing scenario and select new active nodes if necessary. An analysis of this issue requires assumptions on sensor failure phenomenon and is out of the purpose of this paper. Therefore it is left for future research.

## 7. ACKNOWLEDGEMENTS

We thank prof. Sussman for the permission to modify the Amorphous Gray-Scott simulator applet [2].

## 8. REFERENCES

- [1] Amorphous Computing Homepage. <http://www-swiss.ai.mit.edu/projects/amorphous/>.
- [2] The Amorphous Gray-Scott Simulator. <http://www-swiss.ai.mit.edu/projects/amorphous/jsim/sim/GrayScott.html>.

- [3] J. Beal and J. Bachrach. Infrastructure for engineered emergence on sensor/actuator networks. *IEEE Intelligent Systems*, 21(2):10–19, 2006.
- [4] S. Dormann. *Pattern Formation in Cellular Automaton Models - Characterisation, Examples and Analysis*. PhD thesis, University of Osnabrück, Dept. of Mathematics/Computer Science, 2000.
- [5] D. Ganesan, A. Cerpa, W. Ye, Y. Yu, J. Zhao, and D. Estrin. Networking issues in wireless sensor networks. *J. Parallel Distrib. Comput.*, 64(7):799–814, 2004.
- [6] T. C. Henderson, M. Dekhil, S. Morris, Y. Chen, and W. B. Thompson. Smart Sensor Snow. In *IEEE Conference on Intelligent Robots and Intelligent Systems*, pages 1377–1382, 1998.
- [7] J. Hill, R. Szewczyk, A. Woo, S. Hollar, D. Culler, and K. Pister. System architecture directions for networked sensors. In *Proc. of ASPLOS-IX*, pages 93–104, New York, NY, USA, 2000. ACM Press.
- [8] H. Meinhardt. *Models of biological pattern formation*. Academic Press, London, 1982.
- [9] J. D. Murray. Spatial Pattern Formation with Reaction Diffusion Systems, II. In *Mathematical Biology*, volume 18. Springer, New York.
- [10] D. Stoyan, W. S. Kendall, and J. Mecke. *Stochastic Geometry and Its Applications*, page 83. John Wiley & Sons, 1995.